

Received 7 November 2022, accepted 16 November 2022, date of publication 21 November 2022,  
date of current version 30 November 2022.

Digital Object Identifier 10.1109/ACCESS.2022.3223731

## RESEARCH ARTICLE

# Design and Comparison of Different Types of Dual-Frequency Matching Networks Used in Double-Tuned Coils for Multinuclear Magnetic Resonance Imaging and Spectroscopy

CHANG-HOON CHOI<sup>1</sup>, SUK-MIN HONG<sup>1</sup>, N. JON SHAH<sup>1,2,3,4,5</sup>,  
AND JÖRG FELDER<sup>1,5</sup>, (Member, IEEE)

<sup>1</sup>Institute of Neuroscience and Medicine-4, Forschungszentrum Juelich, 52428 Juelich, Germany

<sup>2</sup>Institute of Neuroscience and Medicine-11, Forschungszentrum Juelich, 52428 Juelich, Germany

<sup>3</sup>JARA—BRAIN—Translational Medicine, 52056 Aachen, Germany

<sup>4</sup>Department of Neurology, RWTH Aachen University, 52056 Aachen, Germany

<sup>5</sup>RWTH Aachen University, 52056 Aachen, Germany

Corresponding author: Chang-Hoon Choi (c.choi@fz-juelich.de)

This work was supported by the Deutsche Forschungsgemeinschaft (DFG), German Research Foundation, under Grant 491111487.

**ABSTRACT** Multi-resonant RF coils are often used in multinuclear MR imaging and/or spectroscopy experiments, and a large variety of strategies for multi-tuning coils exist. However, designing a multi-tuned coil with good performance is challenging, and improvements in sensitivity are always desirable - particularly on the X-nucleus coil due to the intrinsically lower MR sensitivity of non-proton nuclei. In this work, various dual-frequency matching networks in double-tuned coils are compared, and their effect on the coil performance is investigated. Four different dual-frequency matching networks were designed and constructed with frequency-splitting or -blocking traps, which enable exploration of both proton-1 (<sup>1</sup>H) and sodium-23 (<sup>23</sup>Na) nuclei. Two single-frequency matching networks were also built without any additional lossy components as a reference, and their matchings were set to either the <sup>1</sup>H or the <sup>23</sup>Na frequency. The initial evaluation was conducted on the bench using a network analyser to examine the scattering (S)-parameters and quality factors of the connected RF coils. The performance of the attached matching networks was then further evaluated by measuring the corresponding signal-to-noise ratio (SNR) based on images obtained at a 7 T clinical MRI scanner. It was found that even though the tuning and matching conditions were nearly impeccable in the S-parameters, the actual <sup>1</sup>H SNR decreased significantly due to the inserted traps, whereas the SNRs of the <sup>23</sup>Na frequency were nearly maintained with the added traps and the losses were much less. The dual-frequency matching networks create additional sensitivity loss, which is dependent on the actual implementation of the matching circuit. This is in agreement with previously reported results associated with the evaluation of inserted double-tuning traps for RF coils.

**INDEX TERMS** Coil, double tuned, matching, MRI, MRS, X-nuclei.

## I. INTRODUCTION

The increasing availability of ultra-high field (UHF) magnetic resonance imaging (MRI) systems delivers numerous benefits, especially in terms of the increased signal-to-noise ratio (SNR), which improves the MR image quality and detection sensitivity [1], [2]. This increased sensitivity

The associate editor coordinating the review of this manuscript and approving it for publication was Yi Zhang<sup>1</sup>.

further enables MR experiments that combine the established proton (<sup>1</sup>H) imaging with less abundant non-proton nuclei (X-nuclei), such as sodium-23 (<sup>23</sup>Na) or phosphorus-31 (<sup>31</sup>P). These X-nuclei facilitate access to valuable cellular and metabolic information in the human body to complement the structural / functional information afforded by proton MRI [3], [4], [5], [6], [7]. For example, sodium plays a key role in the sodium-potassium exchange process in living cells and can therefore be used to access and characterise cell

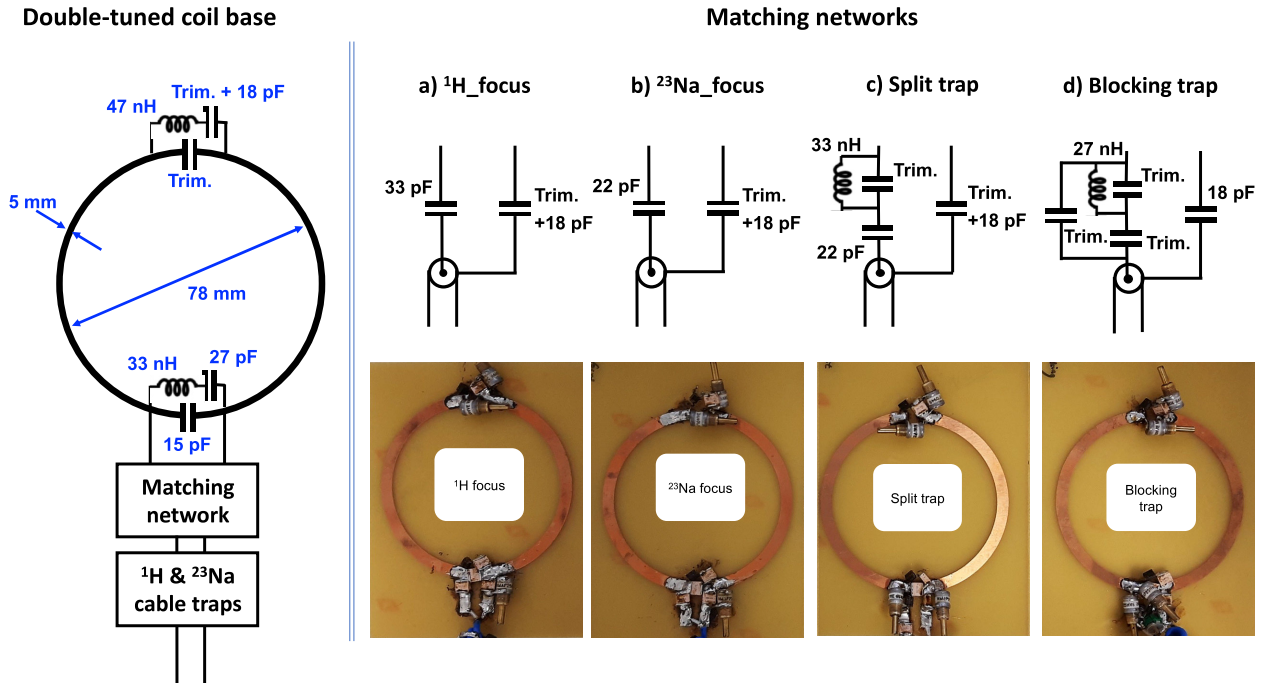


**FIGURE 1.** Schematics of the double-tuned base coil (left). Two single-frequency and two different dual-frequency matching networks inserted on the base coil and their corresponding pictures (bottom right). The matching networks were configured using a)  $^1\text{H}$  focus, b)  $^{23}\text{Na}$  focus, c) frequency-splitting trap, and d) frequency-blocking trap.

metabolism. Moreover, phosphorus shows a strong relation to tissue energy metabolism and determining the quantity of phosphorus metabolites is useful in furthering our understanding of various diseases.

In order to carry out X-nuclei MR imaging or spectroscopic measurements, a radiofrequency (RF) coil and ancillary system that include defined X-nuclei frequencies are explicitly required as the option to operate the X-nuclei experiments is not always integrated in standard MRI systems. Due to the intrinsically lower natural abundance and inferior MR sensitivity of X-nuclei compared to  $^1\text{H}$ , it is important to ensure that the SNR of the X-nuclei remains as high as possible and any improvement in sensitivity on the X-channel is favourable [3]. Thus, a single-tuned X-nucleus coil, assuming no loss, is often used [8].

However, shimming of the main magnetic field, acquiring a rapid localiser image and a high-resolution anatomical image with X-nuclei is problematic due to the low SNR, so concurrent acquisition with proton imaging is advantageous and often necessitated. It is also beneficial to enhance the sensitivity for certain nuclei, e.g.  $^{13}\text{C}$  and  $^{31}\text{P}$ , using the proton-decoupled and / or the nuclear Overhauser effect techniques [9], [10], [11]. Using these methods requires  $^1\text{H}$  signal detection capability to be integrated in the form of a multi-resonant RF coil, which is likely to be utilised for X-nuclei MR studies.

Nevertheless, designing a coil that performs well in this context is challenging, even when it is only required to generate one additional frequency. Double tuning coils requires additional units, and this is usually achieved using various

techniques, e.g. using frequency-splitting or -blocking traps or using PIN-diode switches [12], [13], [14], [15], [16]. The effect of the attached circuits, required for double tuning, on coil sensitivity has been previously reported and has always resulted in a decreased SNR compared to their referenced single-tuned coils [17], [18], [19], [20], [21].

Similar to results previously presented for optimising double-tuned coil designs [12], we anticipate a trade-off, in terms of degree of SNR loss in one resonance against smaller losses in the other, will be encountered in most cases. Although the dual-frequency matching networks can enable a good matching condition by recuperating the impedance mismatch at both frequencies, it can also further engender a level of additional sensitivity degradation. In this regard, a well-designed matching network may be an important criterion when building double- or multi-tuned coils.

To the best of our knowledge, investigating the effect of an inserted dual-frequency or multi-frequency matching network on coil performance has not been carried out, although a study of a double-tuned balun has been presented [21]. In this work, we designed different dual-frequency matching networks and included them in a frequently used, double-tuned coil using inserting traps. We then compared and evaluated the influence of different design approaches.

## II. METHODS

Four identical loop coils were designed and configured in a single structure, as shown in the schematic in Fig. 1 (left). They were double tuned to  $^1\text{H}$  and  $^{23}\text{Na}$  frequencies (corresponding to 297.2 MHz and 78.5 MHz at 7 T, respectively)

using conventional trap circuits without inserting any matching network. By adding the LC trap(s) in the coil, it is typically possible for the single-structure coil to allow multiple resonances [12], [17], [18] by either blocking a particular frequency or splitting one to two or more frequencies. In order to ensure that the quality of the four double-tuned coils was indistinguishable, we measured the quality (Q) factors of the base coils on the bench using a double-sniffer loop [22] and a network analyser prior to adding any matching network. Scattering (S)-parameters were also recorded to describe the coil response, including the tuning and matching conditions of the coil. The reference values were obtained from the double-tuned base coil whereby, for example, in the case of  $^1\text{H}$ \_focus, only the proton frequency was optimised.

Thereafter, the planned matching networks were constructed and implemented in the double-tuned coils as displayed in Fig. 1 (right), which included two single-frequency matching networks without any additional lossy components and the others with two different types of trap circuits. The first two matching networks, i.e.  $^1\text{H}$  focus and  $^{23}\text{Na}$  focus, were assumed as references for evaluation and comparison. To prevent any common mode interference on the cables,  $^1\text{H}$  and  $^{23}\text{Na}$  cable traps were included in each coil and were connected to the MR system via a home-built transmit/receive switches. The matching network,  $^1\text{H}$  focus, in Fig. 1a shows that the matching was only considered at the  $^1\text{H}$  frequency and not at the  $^{23}\text{Na}$  frequency, whereas the matching network,  $^{23}\text{Na}$  focus, in Fig. 1b shows the opposite. In order to achieve good impedance matching for both  $^1\text{H}$  and  $^{23}\text{Na}$  frequencies, the dual-frequency matching networks that were realised using either frequency-splitting or -blocking traps were included, as shown in Fig. 1c and Fig. 1d, respectively. Here, the splitting trap allows current to flow at both the  $^1\text{H}$  and  $^{23}\text{Na}$  frequencies, while the blocking trap restricts one of the frequencies - in our case the  $^1\text{H}$  frequency. The matching conditions of the double-tuned coils with these four different matching networks were then recorded on the bench with and without a 2-litre cylindrical phantom.

A phantom provided by the scanner manufacturer, containing  $3.75 \text{ g NiSO}_4 \times 6\text{H}_2\text{O} + 5 \text{ g NaCl}$  per  $1000 \text{ g H}_2\text{O}$  was used for both the bench measurements and MR experiments. Fig. 2 shows screen-captured S-parameters to demonstrate the matching conditions of the four different matching networks with the phantom. In the case of using matching traps (i.e. splitting and blocking in Fig. 1c and 1d), we were able to achieve matching better than  $-30 \text{ dB}$  at both the  $^1\text{H}$  and  $^{23}\text{Na}$  frequencies. However, the matching for focusing on one nucleus (i.e.  $^1\text{H}$  focus and  $^{23}\text{Na}$  focus in Fig. 1a and 1b) only achieved a good matching condition at only one frequency.

The performance of the double-tuned coils with different matching networks was further evaluated using a 7 T MRI scanner (Siemens Healthineers, Erlangen, Germany). The  $^1\text{H}$  and  $^{23}\text{Na}$  images in Fig. 3 were acquired using a standard 2D FLASH sequence, and the imaging parameters for  $^1\text{H}$  were repetition time (TR) = 8.6 ms, echo time (TE) = 3.69 ms, number of averages = 1, slice thickness = 1 mm, in-plane

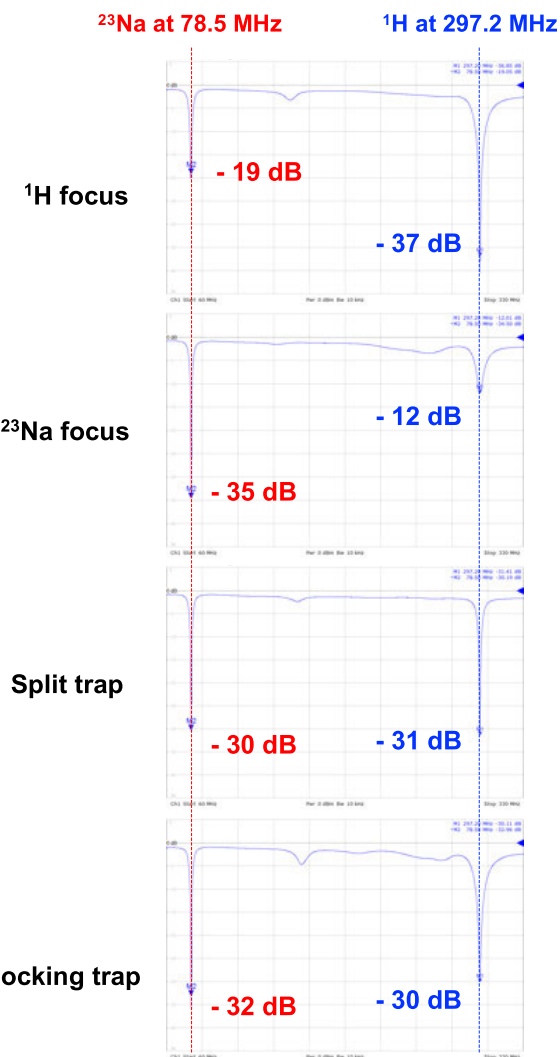


**FIGURE 2.** Screen-captured scattering-parameters ( $S_{11}$ , return loss) of the double-tuned coil with four different dual-frequency matching networks at  $^1\text{H}$  and  $^{23}\text{Na}$  frequencies at 7 T.

resolution =  $0.5 \times 0.5 \text{ mm}^2$ , matrix size =  $256 \times 256$  and acquisition time = 10 seconds, and for  $^{23}\text{Na}$  - TR = 150 ms, TE = 3.34 ms, number of averages = 24, slice thickness = 5 mm, in-plane resolution =  $3 \times 3 \text{ mm}^2$ , matrix size =  $64 \times 64$  and acquisition time = 2:53 minutes. For the SNR calculations, transmit (Tx) powers were calibrated using a variable flip angle method and the noise images were acquired without Tx (Tx = 0 V), according to the NEMA method [23]. Although magnitude images were used to compute the mean of the noise power, the correction factor for the Rayleigh distribution of noise in the magnitude images was not applied as only relative values are of interest.

### III. RESULTS

The Q-factors of the four foundation double-tuned coils were: unloaded Q  $\sim 100$  for  $^1\text{H}$  and  $\sim 240$  for  $^{23}\text{Na}$ , loaded Q  $\sim 50$  for  $^1\text{H}$  and  $\sim 140$  for  $^{23}\text{Na}$  and unloaded/loaded Q ratio  $\sim 2$  for  $^1\text{H}$  and  $\sim 1.7$  for  $^{23}\text{Na}$ , confirming that there was

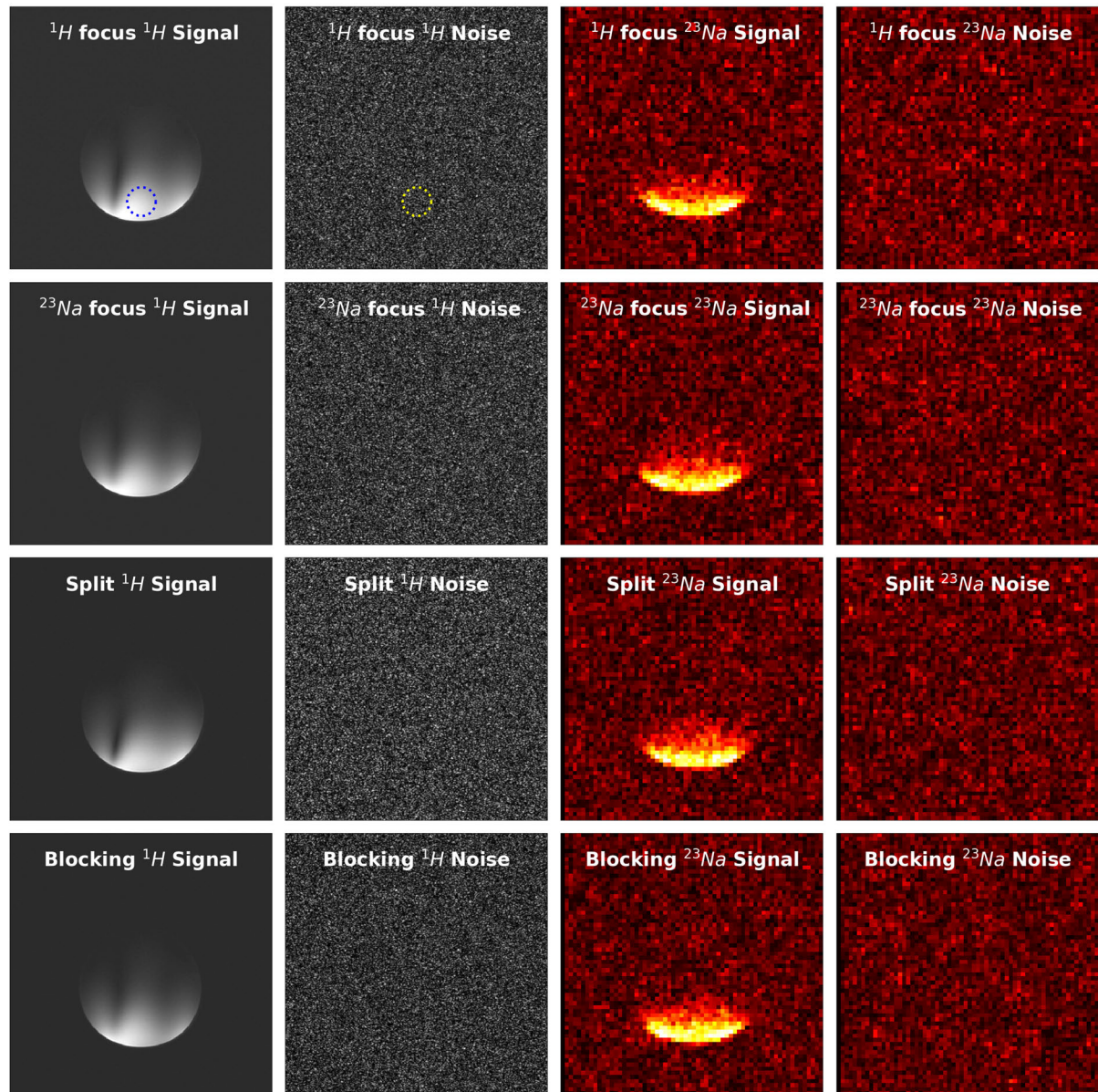


**FIGURE 3.**  $^1\text{H}$  (left column, grey colour) and  $^{23}\text{Na}$  (right column, hot colour) MR images acquired using the different matching networks. These were used to calculate the SNR values (signal mean/noise standard deviation) at the region of interest. The selected signal (blue dotted circle) and noise (yellow dotted circle) regions are shown in the  $^1\text{H}$  focus images. The noise images were obtained with the transmit power of 0 V.

no significant quality difference among the base coils within experimental error.

Fig. 3 shows  $^1\text{H}$ ,  $^1\text{H}$  noise,  $^{23}\text{Na}$  and  $^{23}\text{Na}$  noise images acquired by means of the different matching networks. Using these images, the relative SNRs were calculated in the selected region-of-interest (blue dotted circle in the  $^1\text{H}$  focus image and yellow dotted circle in the  $^1\text{H}$  focus noise image).

The calculated SNR values for  $^1\text{H}$  and  $^{23}\text{Na}$  are summarised in Table 1. As anticipated, the reference coils focusing only on either  $^1\text{H}$  or  $^{23}\text{Na}$  without the addition of dual-frequency matching networks provided the highest SNR: 313.9 for  $^1\text{H}$  and 13.4 for  $^{23}\text{Na}$ . These values were used as a baseline to evaluate the SNR changes resulting from

the inclusion of the splitting and blocking traps. Table 1 also shows that the  $^{23}\text{Na}$  SNR degradation by the added splitting or blocking traps is not quite significant but that of  $^1\text{H}$  focus is much higher (up to 22% loss), while the  $^1\text{H}$  SNR degradation by the inserted traps is quite significant (up to 20% loss) but that of  $^{23}\text{Na}$  focus is much less ( $\sim 9\%$ ). Importantly, even though the tuning and matching conditions were nearly impeccable in the S-parameters, the actual SNR dropped substantially, particularly at the  $^1\text{H}$  channel, as a result of the insertion of splitting or blocking traps. On the other hand, when compared to the reference, the SNRs of the  $^{23}\text{Na}$  channel were nearly maintained with the added traps and the losses were much less. The SNRs of the  $^1\text{H}$  images seem to be more

TABLE 1. Calculated SNR values.

Matching type	$^1\text{H}$ SNR	Percentage to $^1\text{H}$ focus	$^{23}\text{Na}$ SNR	Percentage to $^{23}\text{Na}$ focus
$^1\text{H}$ focus	313.9	100.0% (= 313.9/313.9)	10.5	78.4% (= 10.5/13.4)
$^{23}\text{Na}$ focus	287.6	91.6% (= 287.6/313.9)	13.4	100.0% (= 13.4/13.4)
Splitting	264.9	84.4% (= 264.9/313.9)	12.4	92.5% (= 12.4/13.4)
Blocking	251.2	80.0% (= 251.2/313.9)	12.8	95.5% (= 12.8/13.4)

affected by the inserted traps. Interestingly, the coil focusing on  $^{23}\text{Na}$  only provided much better SNR for  $^1\text{H}$ , although the coil was not ideally but reasonably matched at the  $^1\text{H}$  frequency, which might be due to perhaps the exclusion of lossy components.

#### IV. DISCUSSION

This study focuses on the insertion of different dual-frequency matching networks in a single-structure, double-tuned  $^1\text{H}/^{23}\text{Na}$  coil and compares their effect on the coil performance. This single-structure configuration is widely used since it simplifies the multi-channel extension as it does not require decoupling between nuclei within each channel and it guarantees the identical imaging field-of-view between both nuclei, enabling a straightforward post-acquisition image co-registration [12].

In general, the traditional LC traps used in double-tuned coils are lossy and degrade the quality and SNR of the coil by approximately 25% at either channel or both channels when compared to the single-tuned coil [19]. Comparable results were found in this work with the dual-frequency matching networks designed using the frequency-splitting or -blocking traps. It has also been reported that the level of degradation could be balanced at both nuclei or weighted to one of the nuclei by adjusting the value of the selected inductor in the traps [20], [24]. This means that the improvement in the quality of the non-proton channel may be traded off with that of the  $^1\text{H}$ , and this can also be further optimised to make it as good as that of the single-tuned coil [25].

Tuning and matching the coil on the imaging object is a final step to complete coil construction. While this appears to be an ordinary step, it is essential since this clearly determines the most efficient RF power transfer between the coil and the loaded object and influences the MR image or spectrum quality. As shown previously, we found that the design -  $^{23}\text{Na}$  focus - provided the least loss at the  $^1\text{H}$  frequency and the highest SNR at the  $^{23}\text{Na}$  frequency when the coil was only tuned and matched well at the  $^{23}\text{Na}$  frequency. This suggests that the optimisation of tuning and matching in all the nuclei of interest using, e.g. the dual-frequency matching networks, may not be required in order to improve the quality of multinuclear MR imaging and spectroscopy. Investigating other approaches introduced in double-tuned coils, e.g. using PIN-diodes [25], [26] or LCC trap circuits [27], [28] would also be useful, as these might provide less degradation in the

coil sensitivity. It would also be of interest to explore whether the matching networks for coils operating at close frequencies (e.g.  $^1\text{H}/^{19}\text{F}$  or  $^{13}\text{C}/^{23}\text{Na}$ ) or at other frequencies that are far apart from  $^1\text{H}$  (e.g.  $^{17}\text{O}$  or  $^{39}\text{K}$ ) are affected in a similar way.

Here, we have primarily chosen a loop coil design for demonstration as this is one of the most frequently used configurations. As field strength increases to ultra-high field, radiating antennas become popular since they reduce the problems associated with a shortened RF wavelength and asymmetric pattern when using the traditional loop coils [29], [30], [31]. However, for these antennas, different approaches may be required in terms of reconfiguring the baluns to adjust the matching conditions of the two different nuclei [21].

#### V. CONCLUSION

In conclusion, we have redesigned frequently used dual-frequency matching networks and demonstrated the effect of adding matching networks on a single-structure, double-tuned coil. In agreement with previous results in the literature associated with the evaluation of inserted double-tuning traps, the dual-frequency matching networks also create additional sensitivity loss to some extent. Therefore, it is important to choose a suitable matching network when designing double- or multi-tuned coils in order to minimise any possible loss or degradation in quality.

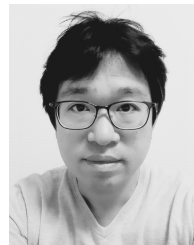
#### ACKNOWLEDGMENT

The authors would like to thank Claire Rick for English proofreading.

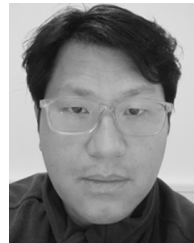
#### REFERENCES

- [1] M. E. Ladd, P. Bachert, M. Meyerspeer, E. Moser, A. M. Nagel, D. G. Norris, S. Schmitter, O. Speck, S. Straub, and M. Zaiss, "Pros and cons of ultra-high-field MRI/MRS for human application," *Prog. Nucl. Magn. Reson. Spectrosc.*, vol. 109, pp. 1–50, Dec. 2018.
- [2] O. Kraff, A. Fischer, A. M. Nagel, C. Mönninghoff, and M. E. Ladd, "MRI at 7 Tesla and above: Demonstrated and potential capabilities," *J. Magn. Reson. Imag.*, vol. 41, no. 1, pp. 13–33, Jan. 2015.
- [3] W. A. Worthoff, A. Shymanskaya, C.-H. Choi, J. Felder, A. Oros-Peusquens, and N. J. Shah, "Multinuclear MR imaging and spectroscopy," in *Quantitative MRI of the Brain*. Boca Raton, FL, USA: CRC Press, 2018.
- [4] M. Modo, " $^{19}\text{F}$  magnetic resonance imaging and spectroscopy in neuroscience," *Neuroscience*, vol. 474, p. 37050, Oct. 2021.
- [5] D. Paech, A. M. Nagel, M. N. Schultheiss, R. Umathum, S. Regnery, M. Scherer, A. Wick, T. Platt, W. Wick, M. Bendszus, A. Unterberg, H.-P. Schlemmer, M. E. Ladd, and S. C. Niesporek, "Quantitative dynamic oxygen 17 MRI at 7.0 T for the cerebral oxygen metabolism in glioma," *Radiology*, vol. 295, no. 1, pp. 181–189, Apr. 2020.

- [6] A. Rietzler, R. Steiger, S. Mangesius, L.-M. Walchhofer, R. M. Gothe, M. Schocke, E. R. Gizewski, and A. E. Grams, "Energy metabolism measured by  $^{31}\text{P}$  magnetic resonance spectroscopy in the healthy human brain," *J. Neuroradiol.*, vol. 49, no. 5, pp. 370–379, Sep. 2022.
- [7] C. Kopp, P. Linz, L. Wachsmuth, A. Dahlmann, T. Horbach, C. Schöfl, W. Renz, D. Santoro, T. Niendorf, D. N. Müller, M. Neining, A. Cavallaro, K.-U. Eckardt, R. E. Schmieder, F. C. Luft, M. Uder, and J. Titze, " $^{23}\text{Na}$  magnetic resonance imaging of tissue sodium," *Hypertension*, vol. 59, no. 1, pp. 167–172, 2012.
- [8] C.-H. Choi, Y. Ha, P. Veeraiyah, J. Felder, K. Möllenhoff, and N. J. Shah, "Design and implementation of a simple multinuclear MRI system for ultra high-field imaging of animals," *J. Magn. Reson.*, vol. 273, pp. 28–32, Dec. 2016.
- [9] N. Sailasuta, L. W. Robertson, K. C. Harris, A. L. Gropman, P. S. Allen, and B. D. Ross, "Clinical NOE  $^{13}\text{C}$  MRS for neuropsychiatric disorders of the frontal lobe," *J. Magn. Reson.*, vol. 195, pp. 25–219, Dec. 2008.
- [10] T. H. Peeters, M. J. van Uden, A. Rijpma, T. W. J. Scheenen, and A. Heerschap, " $^{3\text{D}}$   $^{31}\text{P}$  MR spectroscopic imaging of the human brain at 3 T with a  $^{31}\text{P}$  receive array: An assessment of  $^1\text{H}$  decoupling,  $T_1$  relaxation times,  $^1\text{H}$ - $^{31}\text{P}$  nuclear overhauser effects and  $\text{NAD}^+$ ," *NMR Biomed.*, vol. 34, p. e4169, Sep. 2021.
- [11] J. Ren, A. D. Sherry, and C. R. Malloy, "Band inversion amplifies  $^{31}\text{P}$ - $^{31}\text{P}$  nuclear overhauser effects: Relaxation mechanism and dynamic behavior of ATP in the human brain by  $^{31}\text{P}$  MRS at 7 T," *Magn. Reson. Med.*, vol. 77, no. 4, pp. 1409–1418, Apr. 2017.
- [12] C.-H. Choi, S.-M. Hong, J. Felder, and N. J. Shah, "The state-of-the-art and emerging design approaches of double-tuned RF coils for X-nuclei, brain MR imaging and spectroscopy: A review," *Magn. Reson. Imag.*, vol. 72, pp. 103–116, Oct. 2020.
- [13] B. C. Rowland, I. D. Driver, M. Tachrount, D. W. J. Klomp, D. Rivera, R. Forner, A. Pham, M. Italiaander, and R. G. Wise, "Whole brain  $^{31}\text{P}$  MRSI at 7T with a dual-tuned receive array," *Magn. Reson. Med.*, vol. 83, pp. 75–765, Aug. 2020.
- [14] S. Ha, M. J. Hamamura, O. Nalcioglu, and L. T. Muftuler, "A PIN diode controlled dual-tuned MRI RF coil and phased array for multi nuclear imaging," *Phys. Med. Biol.*, vol. 55, no. 9, pp. 600–2589, 2010.
- [15] F. Wetterling, M. Tabbert, S. Junge, L. Gallagher, I. M. Macrae, and A. J. Fagan, "A double-tuned  $^1\text{H}/^{23}\text{Na}$  dual resonator system for tissue sodium concentration measurements in the rat brain via Na-MRI," *Phys. Med. Biol.*, vol. 55, pp. 95–7681, Nov. 2010.
- [16] S.-M. Hong, C.-H. Choi, N. J. Shah, and J. Felder, "Design of a double-resonant helmet coil for  $^1\text{H}/^{31}\text{P}$  at 3T MRI of the brain," *Phys. Med. Biol.*, vol. 64, Jan. 2019, Art. no. 035003.
- [17] M. D. Schnell, V. Harihara Subramanian, J. S. Leigh, and B. Chance, "A new double-tuned probe for concurrent  $^1\text{H}$  and  $^{31}\text{P}$  NMR," *J. Magn. Reson.*, vol. 65, no. 1, pp. 122–129, Oct. 1985.
- [18] G. B. Matson, P. Vermathen, and T. C. Hill, "A practical double-tuned  $^1\text{H}/^{31}\text{P}$  quadrature birdcage head coil optimized for  $^{31}\text{P}$  operation," *J. Magn. Reson.*, vol. 42, pp. 82–173, Oct. 1999.
- [19] M. Alecci, S. Romanzetti, J. Kaffanke, A. Celik, H. P. Wegener, and N. J. Shah, "Practical design of a 4 Tesla double-tuned RF surface coil for interleaved  $^1\text{H}$  and  $^{23}\text{Na}$  MRI of rat brain," *J. Magn. Reson.*, vol. 181, pp. 11–203, Aug. 2006.
- [20] A. Dabirzadeh and M. P. McDougall, "Trap design for insertable second-nuclei radiofrequency coils for magnetic resonance imaging and spectroscopy," *Concepts Magn. Reson. B, Magn. Reson. Eng., Educ. J.*, vol. 35, no. 3, pp. 32–121, 2009.
- [21] Y. Zhu, C. R. Sappo, W. A. Grissom, J. C. Gore, and X. Yan, "Dual-tuned lattice balun for multi-nuclear MRI and MRS," *IEEE Trans. Med. Imag.*, vol. 41, no. 6, pp. 1420–1430, Jun. 2022.
- [22] L. Darrasse and G. Kassab, "Quick measurement of NMR-coil sensitivity with a dual-loop probe," *Rev. Sci. Instrum.*, vol. 64, no. 7, pp. 1841–1844, 1993.
- [23] *Determination of Signal-to-Noise Ratio (SNR) in Diagnostic Magnetic Resonance Imaging*, NEMA, Standards MS 1-2008, 2021.
- [24] G. Isaac, M. D. Schnell, R. E. Lenkinski, and K. Vogege, "A design for a double-tuned birdcage coil for use in an integrated MRI/MRS examination," *J. Magn. Reson.*, vol. 89, no. 1, pp. 41–50, 1990.
- [25] C.-H. Choi, S.-M. Hong, Y. Ha, and N. J. Shah, "Design and construction of a novel  $^1\text{H}/^{19}\text{F}$  double-tuned coil system using PIN-diode switches at 9.4 T," *J. Magn. Reson.*, vol. 279, pp. 11–15, Jun. 2017.
- [26] Y. Ha, C.-H. Choi, and N. J. Shah, "Development and implementation of a PIN-diode controlled, quadrature-enhanced, double-tuned RF coil for sodium MRI," *IEEE Trans. Med. Imag.*, vol. 37, no. 7, pp. 31–1626, Jul. 2018.
- [27] M. Meyerspeer, E. S. Roig, R. Gruetter, and A. W. Magill, "An improved trap design for decoupling multinuclear RF coils," *Magn. Reson. Med.*, vol. 72, pp. 90–584, Sep. 2014.
- [28] T. A. van der Velden, M. Italiaander, W. J. M. van der Kemp, A. J. E. Raaijmakers, A. M. T. Schmitz, P. R. Luijten, V. O. Boer, and D. W. J. Klomp, "Radiofrequency configuration to facilitate bilateral breast  $^{31}\text{P}$  MR spectroscopic imaging and high-resolution MRI at 7 Tesla," *Magn. Reson. Med.*, vol. 74, no. 6, pp. 1803–1810, Dec. 2015.
- [29] S. M. Hong, J. H. Park, M. K. Woo, Y. B. Kim, and Z. H. Cho, "New design concept of monopole antenna array for UHF 7T MRI," *Magn. Reson. Med.*, vol. 71, no. 5, pp. 1944–1952, May 2014.
- [30] A. J. E. Raaijmakers, M. Italiaander, I. J. Voogt, P. R. Luijten, J. M. Hoogduin, D. W. J. Klomp, and C. A. T. van den Berg, "The fractionated dipole antenna: A new antenna for body imaging at 7 Tesla," *Magn. Reson. Med.*, vol. 75, pp. 1366–1375, May 2016.
- [31] C.-H. Choi, S.-M. Hong, J. Felder, L. Tellmann, J. Scheins, E. R. Kops, C. Lerche, and N. J. Shah, "A novel J-shape antenna array for simultaneous MR-PET or MR-SPECT imaging," *IEEE Trans. Med. Imag.*, vol. 41, no. 5, pp. 1104–1113, May 2022.



**CHANG-HOON CHOI** received the Ph.D. degree in MRI physics from the University of Aberdeen, Aberdeen, U.K., in 2010. He was at MR Solutions Ltd., Guildford, U.K., until 2014. He is an MR Expert and has been a Senior Scientist with Forschungszentrum Juelich, Germany, since 2014.



**SUK-MIN HONG** received the Ph.D. degree in medical science from Gachon University, South Korea, in 2013. He was at the Neuroscience Research Institute, South Korea, until 2014. He is an RF Coil Expert and has been a Researcher with Forschungszentrum Juelich, Germany, since 2014.



**N. JON SHAH** received the Ph.D. degree from the University of Manchester. He worked on the development of methods for MRI and spectroscopy, Japan. He was at the University of Cambridge on MR and then in Germany, where he is with the Forschungszentrum Juelich. Currently, he is the Director of the Institute of Neuroscience and Medicine-4 and -11, Juelich, a Professor of MRI physics with RWTH, Aachen, and an Adjunct Professor with the MBI, Melbourne.



**JÖRG FELDER** (Member, IEEE) received the Diploma degree in electrical engineering and the doctoral degree from RWTH Aachen University, Aachen, Germany, in 1998 and 2004, respectively. From 2004 to 2007, he was an RF Engineer for Bruker BioSpin MRI GmbH, Ettlingen, Germany. Since 2007, he has been a Team Leader with the Forschungszentrum Juelich, Germany.

•••